Blockchain-Based Route Selection With Allocation of Radio and Computing Resources for Connected Autonomous Vehicles

Marcel Vološin, Eugen Šlapak, Zdenek Becvar, *Senior Member, IEEE*, Taras Maksymyuk, *Member, IEEE*, Adam Petík, Madhusanka Liyanage, *Senior Member, IEEE*, and Juraj Gazda

***Abstract*— With the advent of connected and autonomous vehicles (CAVs), we observe a growing need for new resource allocation solutions in mobile networks. Currently, most of the resource allocation solutions for CAVs communication do not consider the driving routes of the cars. In this paper, we introduce joint vehicular route selection and radio and computing resource allocation for CAVs. The proposed approach is based on the graph search-based lexicographic A* algorithm that minimizes the ratio of failed tasks along the entire vehicular route considering the availability of both radio and computing resources. To manage the allocation of resources among multiple CAVs for each vehicular route, we develop a blockchain-based framework allowing resource reservation by means of nonfungible tokens (NFTs). Each NFT represents an exclusive right to the required amount of radio and computing resources for the given road segment and defined time interval. The effectiveness of the proposed approach is demonstrated by simulations showing that the proposed vehicular route selection algorithm reduces the ratio of tasks not completed before the deadline by up to 69% compared to the existing state-of-the-art algorithms.**

***Index Terms*— Resource allocation, vehicular edge computing, mobile networks, connected vehicles, NFT, blockchain.**

I. Introduction

THE Internet of Things (IoT) era has shifted the paradigm of city development towards digitalization and novel information services based on artificial intelligence (AI) and blockchain. One of the areas of most active development is the automotive industry, which is rapidly transforming towards connected and autonomous vehicles (CAVs). Such CAVs typically contain various supplementary systems, such as sensors, lidars, or global electronic assistance systems. All these supplementary systems generate a massive amount of data and heavily rely on vehicle-to-infrastructure (V2I) communications. An additional complexity of CAV scenarios, for example, autonomous driving, is that a significant percentage of the data is transferred to an external cloud or multi-access edge computing (MEC) servers [1]. By leveraging MEC capabilities, CAVs are capable of increasing the computation efficiency and reducing both, traffic congestion and traffic accidents, respectively. However, despite the availability of the large computational storages provisioned in MEC as well as high-speed data links provided by fifth-generation (5G) mobile network, the autonomous mobility of CAVs remains still the critical challenge for the emerging intelligent transportation systems [2], [3].

The 5G mobile network standards enable ultra-reliable low-latency communications and network slicing to facilitate the adoption of CAVs. The network slicing functionality allows the radio resources of CAVs to be separated from those of other users [4]. However, in addition to radio resource allocation, the allocation of edge computing resources is also vital to meet the low latency requirements of CAVs. Thus, the optimization of radio and computing resources should be considered jointly [5].

CAVs typically move over much larger distances than pedestrians, and the allocated resources should be available along the entire vehicular route of the trip. Thus, the main problem studied in this paper is related to the vehicular routing strategy for CAVs considering the reliability of network connectivity and the availability of computing resources to ensure low latency of computing task processing. The most basic solution for the navigation of vehicles is the selection of the fastest possible route (FPR) [6]. The FPR approach selects the fastest vehicular route between specified origin and destination points based solely on the conventional Global Positioning System (GPS). Navigation systems based on this approach often consider additional parameters, such as traffic jams, speed limits and overall road conditions. However, while FPR selection can be optimal from the perspective of driving time, it is not always good from the perspective of wireless connectivity or computing resource availability, which may be

Manuscript received 22 July 2022; revised 20 December 2022; accepted 3 March 2023. Date of publication 16 March 2023; date of current version 7 July 2023. This work was supported in part by the Science Foundation Ireland under CONNECT Phase 2 under Grant 13/RC/2077_P2; in part by the Ukrainian Government "Designing the Novel Decentralized Mobile Network Based on Blockchain Architecture and Artificial Intelligence for 5G/6G Development in Ukraine," under Project b-0120U100674; in part by the Ministry of Education, Youth and Sports, Czech Republic, under Project LUASK22064; and in part by the Slovak Research and Development Agency under Project SK-CZ-RD-21-0028, Project APVV-18-0214, and Project APVV-21-0318. The Associate Editor for this article was A. H. Sodhro. *(Corresponding author: Juraj Gazda.)*

Marcel Vološin, Eugen Šlapak, Adam Petík, and Juraj Gazda are with the Department of Computer and Informatics, Technical University of Košice, 04200 Kosice, Slovakia (e-mail: juraj.gazda@tuke.sk).

Zdenek Becvar is with the Department of Telecommunication Engineering, Faculty of Electrical Engineering, Czech Technical University in Prague, 166 27 Prague, Czech Republic (e-mail: zdenek.becvar@fel.cvut.cz).

Taras Maksymyuk is with the Department of Telecommunications, Lviv Polytechnic National University, 79000 Lviv, Ukraine (e-mail: taras.maksymyuk@gmail.com).

Madhusanka Liyanage is with the School of Computer Science, University College Dublin, Dublin 4, D04 C1P1 Ireland (e-mail: madhusanka@ucd.ie).

Digital Object Identifier 10.1109/TITS.2023.3255301

essential for the autonomous driving scenario. Under certain conditions, the vehicle may require essential information from the surrounding environment to ensure a safe and comfortable trip.

Thus, there is a critical need to propose a scalable routing algorithm that addresses the joint optimization of radio and computing resources to ensure the seamless generation of various service requests by CAVs in the MEC environment [7]. In addition, the route selection mechanism must be designed such that the route prolongation of the CAVs falls within a specific acceptable threshold. Decentralized solutions are of prominent interest considering the presence of a large number of CAVs and their high mobility, which could impose high time and memory requirements on the typical centralized solutions presented in, e.g. [8] and [9].

To fill this research gap, in this paper, we propose a novel blockchain-based framework for vehicular route selection. Unlike related works, we consider jointly the end-to-end radio and computing resource availability. The motivation for blockchain implementation is the distributed ledger, which provides decentralized trust and secure interaction without any central authority. In the context of resource sharing, we use blockchain to track the corresponding gNodeB (gNB) resource allocation agreements of the gNBs and to ensure that each CAV experiences the expected quality of service (QoS). This is achieved by means of nonfungible tokens (NFTs), which are linked to the reservation of the radio and computing resources of the gNBs. The main contributions of this paper are summarized as follows:

1) We propose a novel vehicular route selection algorithm for CAVs based on the A* search algorithm with a modified heuristic function to minimize the ratio of failed computing tasks in the autonomous driving scenario by considering the availability of both radio and computing resources along the entire vehicular route.
2) We develop a blockchain-based framework for joint radio and computing resource allocation and NFT-based reservation of radio and computing resources over the whole journey of CAVs.
3) We demonstrate that the proposed vehicular route selection strategy significantly outperforms the state-of-the-art solutions in terms of the failed computing task ratio and paves the way for the deployment of CAV in the future.

In summary, we provide the novel application of the A* graph search algorithm to determine the CAV route selection in the autonomous driving scenario, where the aim is to minimize the number of tasks not completed before the deadline. The route selection is determined based on the available radio and computing resources in the individual road segments, which are in turn reserved for the particular CAV by issuing NFTs over the blockchain platform. Consequently, when CAV reaches the target road segment, it can use the pre-allocated radio and computing resources, resulting in a decrease in the failed task ratio compared to the state-of-the-art works.

The remainder of this paper is organized as follows. Section II provides some background and an overview of related works on MEC-based vehicular communications, blockchain and vehicular routing mechanisms. Section III introduces the system model considered in this paper. Section IV presents a detailed explanation of the proposed joint vehicular route selection and resource allocation algorithm. Section V discusses the simulation and performance evaluation of the proposed approach in comparison to state-of-the-art solutions. We conclude our paper by suggesting some general directions for further research in Section VI.

II. Background and Related Work

In this section, we provide some background and an overview of related works on vehicular communications based on MEC, blockchain applications in vehicular MEC networks and vehicular routing mechanisms leveraging MEC.

A. MEC in a Vehicular Environment

The computational part of vehicular services plays a crucial role in the overall user experience. Most advanced applications of CAVs require significant amounts of data processing, caching and storage, which should be instantly available on the fly to ensure a comfortable and safe driving experience while avoiding traffic accidents. Although critical data are processed locally, each CAV requires additional data processing at neighbouring edge servers, which can solve more complex but less urgent tasks [10]. Therefore, MEC is seen as a key enabler of edge intelligence and low-latency computing capabilities for CAVs. The authors of [11] propose an algorithm for computing resource allocation in MEC under decoupled latency/resource constraints. The authors leverage particle swarm optimization to solve the unconstrained optimization problem. In [12], a collaborative virtual MEC framework formed by a cluster of CAVs is presented that takes advantage of the determined CAVs' mobility. However, only the computing capabilities of the virtual MEC framework are analysed while excluding the radio part from the scope of the analysis. In [13], the authors propose a heuristic adaptive radio resource allocation strategy for computation offloading. The authors focus primarily on the radio resource allocation strategy considering various levels of CAV mobility. A task scheduling pricing model in a collaborative MEC framework based on the application of contract theory and prospect theory is developed in [14]. Finally, a complex techno-economic cost analysis of MEC deployment aiming to provide full network coverage for CAVs is presented in [15]. All these papers demonstrate the effectiveness of MEC for CAVs. However, none of these works leverages MEC for advanced CAV route selection, and the role of the mobility patterns of the CAVs is limited; they serve only as the internal stimuli for the dynamic resource scheduling of radio and/or computing resources.

B. Blockchain-Empowered V2I Solutions

Blockchain allows the decentralized transfer of value in a secure and mutually trusted way [16]. Such features make blockchain an attractive solution for improving the security and transparency of V2I by deploying a distributed ledger and smart contracts. Blockchain can also be adopted for any type of secure data management and exchange in V2I systems.

For example, blockchain can support trusted data exchange between CAVs and the MEC layer. The authors of [17] propose a blockchain platform for secure data processing addressing various challenges, including CAV mobility and abruptly changing mobility patterns.

The concept is further extended in [18] by incorporating optimization of the radio resources for the blockchain application using reinforcement learning (RL) and treating the optimization process as a multiarmed bandit problem. A novel trust management system based on blockchain for the cooperative verification and storage of sensitive data with the help of MEC is further presented in [19]. From the MEC perspective, blockchain technology can ensure that the data shared by CAVs are legitimate and that each CAV has corresponding permissions to access the computing resources of MEC servers [20], [21]. Finally, from the communication point of view, blockchain can be applied for radio resource sharing, mobility management and the establishment of service level agreements (SLAs) between network operators and CAVs [22], [23]. Although the approach proposed in this paper could be integrated even via third-party product (3PP) applications such as conventional distributed databases, as proposed in [6], there are certain advantages in favour of blockchain. We simultaneously utilize multiple advantages of blockchain as considered in the aforementioned works, as will be revealed in greater detail later in the text.

C. Vehicular Routing and Resource Allocation

Despite the large variety of different solutions for resource allocation in MEC networks, as presented above, most works focusing on the integration of MEC with CAVs consider dynamic resource management as a problem of network adaptation to CAV mobility. In contrast, in our paper, we consider the problem from the CAV side, and we adapt the vehicular routing decisions to the dynamic load variations of the gNBs. In regard to vehicular routing/navigation, the authors of [24] propose a specific mechanism for CAV navigation by means of a low earth orbit (LEO) satellite constellation network to decrease the load pressure on the ground infrastructure. However, this approach can impose additional requirements on the latency. A centralized scheme allowing a hybrid automated planning approach for CAVs is proposed in [25]. The main goal is to prevent congestion. To this end, the network controller balances the traffic in a certain region. Nevertheless, the authors do not address the microscopic attributes of the network in terms of the individual service requests of the CAVs. The work of [24] is further extended in [9], where MEC is considered for traffic route planning and traffic signal planning by leveraging a replicator dynamics model. A signal-to-interference-plus-noise ratio (SINR) quality-based centralized vehicular route selection algorithm (SQRSA) is proposed in [8]. SQRSA selects the vehicular route based on the most feasible SINR map. The long-term average SINR fingerprints for each road segment are stored in a centralized database controller and updated regularly. The vehicular network-aware route selection algorithm (VaRSA) presented in [6] further extends SQRSA with awareness of radio resource availability during driving. Finally, integrated route planning and resource allocation respecting the individual CAV service requests in the MEC context is discussed in [26]. The authors design an offloading policy that minimizes the total service delay. For this purpose, the authors propose interconnected large-scale and small-scale optimization frameworks based on the identification of the Nash equilibrium (NE) for the cost-efficient allocation of radio and computing resources to the CAVs. However, NE identification could be impractical in real use cases, as it requires a priori knowledge of the best response dynamics of the other interacting CAVs.

None of the presented works can ensure continuous service availability in cases of variable network loads and possible congestion of the radio or computing resources. Moreover, to the best of our knowledge, there is currently no solution for vehicular route selection that jointly considers the availability of radio and computing resources to guarantee the end-to-end quality of computing-related services that are essential to the CAVs. In turn, state-of-the-art works still show significant performance gaps in terms of the packet loss ratio and latency, which limit the deployment of CAVs for autonomous driving scenarios. In contrast to the related works, we jointly optimize the radio and computing resource availability in a decentralized manner via blockchain to deliver reliable end-to-end performance in terms of a low failed task ratio while prolonging the travel route only negligibly. The proposed framework paves the way for further advancements in the autonomous mobility domain via the provisioning of a more reliable and scalable routing for CAVs.

III. System Model

In this section, we describe the overall model of the investigated system, including the communication, computing, and latency models, which represent the end-to-end QoS. All mathematical notations used for system model description are defined in Table I. The overall scenario of resource allocation among autonomous CAVs is illustrated in Fig. 1.

We focus on autonomous driving based on V2I communication and computing services. We consider N_{CAV} CAVs and N_{gNB} gNBs in the system. Each gNB is collocated with one MEC server; hence, there are also N_{gNB} servers. As the gNBs and servers are tightly integrated, we will refer to the gNBs as the entities that perform the task processing for conciseness. The communication data rate for offloading a task between the u-th CAV and the s-th gNB is calculated as

$$R_{u,s}(t) = \beta_u(t)\rho_u(t)\ f_{\mathrm{s}}(t)\ \left\lceil \frac{N_{\mathrm{RB}}}{N_{\mathrm{CAV},s}(t)} \right\rceil, \tag{1}$$

where $\beta_u(t)$ represents the number of bits per symbol, $f_{\mathrm{s}}(t)$ is the current symbol rate, $\rho_u(t)$ is the code rate, N_{RB} denotes the total number of resource blocks (RBs) at the s-th gNB, and $N_{\mathrm{CAV},s}(t)$ represents the number of CAVs associated with the s-th gNB at time t. The SINR at time t is mapped to the modulation and coding scheme (MCS) to determine the specific values of β_u and ρ_u in line with [27].

We assume the transmission of high data volumes between the CAVs and gNBs in the uplink direction, whereas the computing output is small in size, so the transmission delay for feedback in the downlink direction is negligible [28]. Hence,

TABLE I
TABLE OF MAIN NOTATIONS USED

Notation	Definition
u	u-th CAV
v	CAV velocity
σ	vehicular route segment
task_i	task identified by index i
D_i	data size of request for task i in MB
$I_{r,i}$	computing rate assigned to task i in IPS
I_{i}	instruction count of task i in MI
$I_{r,\text{CPU}}$	computing rate of a gNB's CPU in IPS
t_{deadline}	latency requirement of task i
$t_{\text{start},i}$	starting time step for task i
$t_{\text{end},i}$	ending time step for task i
Δt_{T}	duration of a traffic simulation time step
$t_{\text{total},i}$	total time consumed for task i
$t_{\text{uplink,i}}$	uplink communication time for task i
$t_{\text{process},i}$	processing time for task i
t_{req}	time of request initiation by a CAV
v_i	i-th graph vertex
v_{destin}	destination graph vertex (route destination)
v_{orig}	origin graph vertex (route origin)
CAND_seg	candidate set of all path segments considered during optimization
CAND_seg_v_i	subset of **CAND_seg** corresponding to vertices v_{orig} to v_i
AR_seg	set of route segments determined via the proposed approach
FPR_seg	set of route segments determined via the FPR approach
t_{rel}	time when requested resources are released
t_{coef}	maximum CAV traversal time prolongation coefficient
$r_i^{\text{uplink}}(t)$	available data rate on uplink channel for i
$B_{\text{W}}^{\text{uplink}}$	bandwidth of uplink wireless channel
$p_{\text{W}}^{\text{uplink}}$	transmission power for uplink wireless channel
$\beta_u(t)$	number of bits per symbol for CAV u
$\rho_u(t)$	code rate for CAV u
f_{s}	symbol rate
R	code rate
N_{CAV}	total number of simulated CAVs
N_{gNB}	number of gNBs
N_{RB}	total number of RBs provided by the s-th gNB
$n_{\text{RB},i}$	number of RBs assigned to the i-th task
$N_{\text{CAV},s}(t)$	number of CAVs connected to the s-th gNB at time t
N_{FT}	total number of failed tasks
N_{GT}	total number of generated tasks
M_{FT}	failed task ratio
T_{AR}	travel time of the vehicular route determined via the proposed algorithm
T_{FPR}	time of the fastest possible vehicular route
M_{RP}	ratio of vehicular route prolongation
D_{O}	route length from its origin to a given v_i
D_{H}	general heuristic function for the distance between v_i and the route destination
D_{M}	Manhattan distance heuristic function from a given v_i to the route destination
$CC_{\text{NFT\_missing}}$	cumulative cost of missing NFTs
CC_{RB}	cumulative cost of reserved RBs
P_{t}	transmission power
f_{t}	carrier frequency

the total time $t_{\text{total},i}$ for offloading the i-th task, encompassing the communication and processing time, is defined as

$$t_{\text{total},i} = t_{\text{uplink},i} + t_{\text{process},i}, \tag{2}$$

where $t_{\text{uplink},i}$ and $t_{\text{process},i}$ represent the delay due to uplink communication from the CAV to the MEC server for the i-th task and the processing time of the i-th task at the MEC server, respectively. These individual task latencies are calculated as

$$\begin{aligned} t_{\text{uplink},i,s} &= D_i / R_{u,s}(t), \\ t_{\text{process},i,s} &= I_i / I_{r,\text{CPU},s}, \end{aligned} \tag{3}$$

where D_i denotes the size of the i-th task as transmitted in the uplink direction, measured in megabytes (MB); I_i is the instruction count of task i, measured in millions of instructions (MI); and $I_{r,CPU,s}$ characterizes the available CPU resources at the associated s-th gNB, which processes the i-th task, in terms of the computing rate in instructions per second (IPS). Note that we do not include the route planning and corresponding blockchain transactions to the total time $t_{\text{total},i}$, as the planning process is executed offline prior to the CAV departure. In addition, we neglect the waiting time that is necessary for the complete proposed solution during the planning stage before departure, since it is not related to the investigated performance metrics and route selection and this time is only in order of milliseconds.

A task is considered successfully solved by the network if the computing result is returned to the CAV within the deadline $t_{\text{deadline},i}$, i.e., if

$$t_{\text{total},i} <= t_{\text{deadline},i}. \tag{4}$$

We define the *failed task ratio* metric to quantify the proportion of tasks for which the latency constraint (4) is not satisfied as

$$M_{\text{FT}} = \frac{N_{\text{FT}}}{N_{\text{GT}}}, \tag{5}$$

where N_{FT} is the number of tasks that fail to be processed within the latency constraint and N_{GT} is the total number of generated tasks.

IV. PROPOSED JOINT VEHICULAR ROUTE SELECTION AND RESOURCE ALLOCATION ALGORITHM

This section formulates the objective function of the considered multiobjective optimization problem and the constraints imposed during optimization. This is followed by a description of the key properties of the proposed blockchain-based solution and a description of the NFT structure. Then, we explain the main components of our proposed vehicular route selection algorithm based on the A* search algorithm while also considering resource allocation aspects. Finally, we describe the resource reservation management mechanism and the key benefits of the blockchain and NFT technology used for this task.

A. Formulation of the Joint Optimization Problem

Our aim is to minimize the failed task ratio M_{FT} and the total traversal time of the vehicular route chosen by a given autonomous CAV. Thus, we formulate the following multiobjective optimization problem, which is composed of

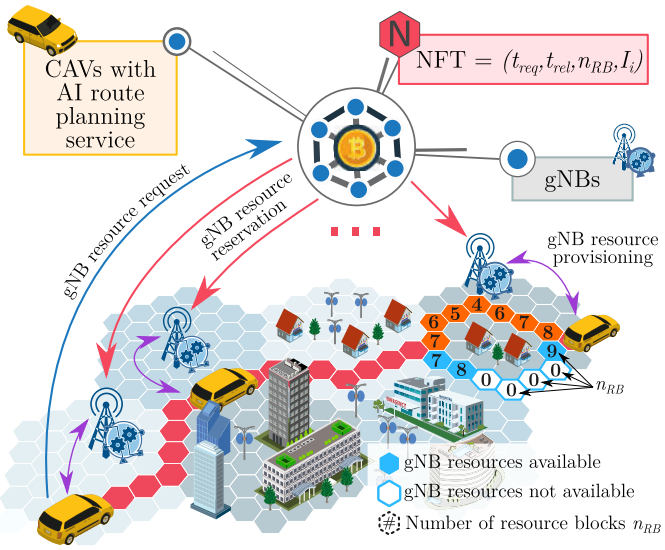

Fig. 1. System model of gNB resource allocation utilizing blockchain. The red hexagonal NFT pictograms jointly denote the graph vertices determining CAV positions (i.e., road segments) and the specific time-varying weights of the associated graph edges. Each weight value is a composite cost consisting of the number of failed tasks for the given route segment, the number of RBs n_{RB}, and the vehicular route length. $\mathrm{NFT}_{\mathrm{missing}}$ is 0 (depicted as a coloured route segment) or 1 (depicted as an empty route segment) depending on gNB resource availability, and n_{RB} is represented as the number inside the hexagon.

two parts:

$$
\begin{aligned}
P1: \quad & \min_{N_{\mathrm{CAV}}, D_i, I_{r,i}, P_{\mathrm{t}}, f_{\mathrm{t}}} \left(M_{\mathrm{FT}}, \sum_{\sigma \in \mathbf{CAND\_seg}} |\sigma|/v \right) \\
& s.t.: \; C1: \sum_i n_{\mathrm{RB},i}\, \alpha(i,s,k) \leq N_{\mathrm{RB}}, \\
& \qquad C2: \sum_i I_i\, \alpha(i,s,k) \leq I_{r,\mathrm{CPU}}, \\
& \qquad C3: \sum_{\sigma \in \mathbf{CAND\_seg}} |\sigma|/v \\
& \qquad \leq \Big(\sum_{\sigma \in \mathbf{FPR\_seg}} |\sigma|/v \Big) * t_{\mathrm{coef}}, \qquad (6)
\end{aligned}
$$

where σ and $|\sigma|$ denote a road segment and its length, respectively; **CAND_seg** and **FPR_seg** represent the candidate set of all route segments and the segments determined via the FPR approach, respectively; v denotes the CAV velocity; and $\alpha(i,s,t)$ returns a value of 1 if the i-th task is associated with the s-th gNB at time t and a value of 0 otherwise.

The solution obtained through the optimization process is subject to the following constraints. *C1* limits the number of RBs that can be requested by all tasks at a given time t to the total number of RBs available at the gNB. *C2* constrains the total computing rate requested by all tasks at a given gNB at time t to the total computing rate provided by the gNB.

C3 upper bounds the total traversal time of the vehicular route chosen by the autonomous CAV to the FPR time multiplied by the coefficient t_{coef}, representing the maximum traversal time prolongation tolerated by the CAV. This parameter reflects the willingness of the passengers travelling in the CAV to trade off a longer route traversal duration for a higher service quality. This preference may be provided by the passengers in advance and treated as one of the known parameters of the CAV.

The defined multiobjective optimization problem includes two parts with different priorities. A feasible solution to this specific optimization problem can be derived via lexicographic optimization, inspired by the A* search algorithm, as shown later in subsection IV-C.

B. Blockchain as a Core Component

A platform implementing resource allocation should be simultaneously reliable, trustworthy, fast, and transparent. Therefore, public blockchain is chosen as the fundamental technological basis of the proposed solution allowing any CAV to join and use the platform with no restrictions after free registration. The utilization of blockchain causes the platform to be decentralized in nature; hence, the reliability and availability of services are increased, as the platform does not rely on a limited set of centralized infrastructure nodes. Of course, a decentralized approach provides resilience and solves the problem of unintentional centralized failure even without blockchain. However, without blockchain, such a decentralized approach would create a large and weakly protected attack surface. As shown in recent studies [29], [30], [31], the computing requirements of blockchain implementation and vehicular network optimization can be fulfilled by the MEC resources collocated with the gNBs, acting as ledger maintainers and transaction verifiers in our concept. Blockchain mitigates security risks such as gNB impersonation [30], denial of service (DoS)/distributed denial of service (DDoS) attacks [32], double spending and data forgery, providing a strong guarantee of accountability [33].

In accordance with the properties of the relevant resources and the nature of their utilization, NFTs are used to store the allocation details and to prove ownership. NFTs were introduced in the ERC-721 standard to provide the feature of uniqueness [34], which is not present in traditional cryptocurrencies, meaning that one NFT is not equivalent to any other NFT [35]. By exploiting this feature, we represent the joint gNB radio and computing resources required by the CAVs at each timestamp as tradable tokens in the digital blockchain ecosystem. These tokens can be purchased by CAVs in advance to ensure the required QoS and avoid outages. To prevent forging attacks, each NFT is signed by the gNB at the time of minting. Only tasks of CAVs with valid associated NFTs are guaranteed to be solved within the required time. The ownership of these digital assets bound to real-world gNB resources can be easily transferred via a free market.

Fig. 2 illustrates the relationships among all building blocks of the proposed concept. The interactions between autonomous CAVs and gNBs that are related to resource allocation are handled by means of smart contracts [36] within the blockchain. The tampering resilience and transparency of the gNB resource reservations stored in the distributed ledger in the form of NFTs are critical for both vehicular route planning and resource utilization.

NFTs play a significant role in our approach, enabling secure and tractable decentralized scheduling of gNB resource

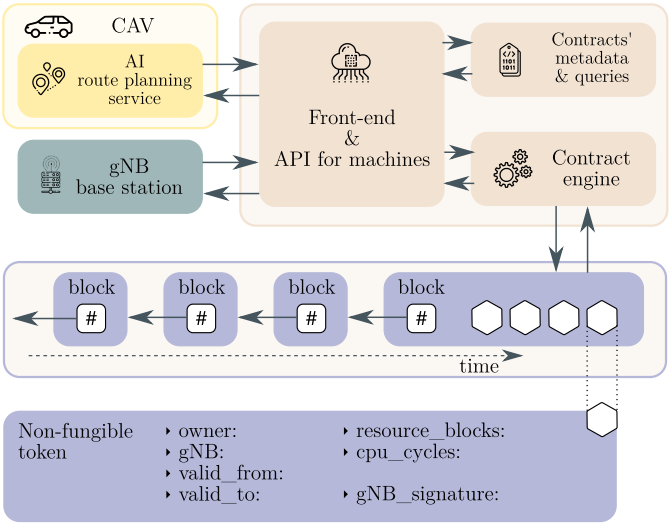

Fig. 2. Overview of decentralized resource allocation with a blockchain core.

allocation. Each NFT necessarily contains a tuple of key parameters describing the resource reservation details:

$$\text{NFT} = (t_{\text{req}}, t_{\text{rel}}, n_{\text{RB},i}, I_i), \tag{7}$$

where t_{req} is the timestamp indicating when the resources of the gNB should be reserved for a given CAV's task and t_{rel} is the timestamp at which the gNB resources can be released. The underlying process of computing the NFT tuple values is described in the following sections.

The defined NFT structure possesses several key features. On the one hand, making t_{req} and t_{rel} flexible allows us to cope with time offsets on a time scale of milliseconds/seconds that can arise due to unpredictable situations in traffic. The CAV can flexibly adjust this time interval to accommodate small-scale time variations to enable instantaneous radio and computing services on a given route segment. On the other hand, when large disruptions in traffic occur and the CAV is unable to reach the target route destination with the reserved NFTs, the CAV can sell its NFT property to another network entity that can utilize it in the given segment and time interval. The blockchain network acts as the intermediary for such NFT exchange, allowing changes in NFT ownership between CAVs and other network entities. By leveraging this feature, we can further enhance the utilization efficiency of the radio and computing resources. However, we leave the consideration of the network economy of such an ecosystem to our future research, and we do not integrate it into our currently proposed solution to avoid losing focus on the topic at hand.

C. Proposed Joint Vehicular Route and Resource Selection Algorithm

To select vehicular routes and allocate radio and computing resources to the CAVs along their individual routes, we develop a solution inspired by the A* routing algorithm. The generic A* algorithm for route selection while minimizing route cost is well established. We choose the lexicographic form of the A* algorithm to avoid unnecessary tuning of the multiobjective tradeoffs since we determine the priority of the multiple metrics to be optimized in advance. By avoiding a search through unnecessary tradeoffs, the lexicographic approach also decreases computational complexity [37], [38].

The algorithm operates on a graph structure G, which consists of graph edges $E(G)$, in our case representing the costs associated with the route segments, and graph vertices $V(G) = v_1, \ldots, v_n$, corresponding to discrete vehicular route locations forming the endpoints of the route segments; accordingly, $E(G) = \{\{v_1, v_2\}, \ldots \{v_{n-1}, v_n\}\}$. The algorithm searches for the path in the graph with the lowest cumulative cost by expanding the vertices $V(G)$. To effectively guide the search through the graph, a cost function should be defined to estimate the total cost of a candidate path through the graph by summing the known edge weights of the explored segments of the candidate path with a heuristically estimated cumulative edge weight of the unexplored segments of the candidate path. Hence, the cost function $f(v_i)$, representing the total estimated path cost of a candidate path passing through a particular v_i, is formulated as

$$f(v_i) = g(v_i) + h(v_i), \tag{8}$$

where $g(v_i)$ is the real cumulative cost of the candidate path from the graph vertex v_{orig} corresponding to the route origin to the i-th vertex v_i and $h(v_i)$ is a heuristic function returning an estimate of the candidate path cost from the given v_i to the graph vertex v_{destin} corresponding to the route destination.

The cost function $g(.)$ constitutes the real cost of the candidate path from v_{orig} to v_i in the form of a triplet:

$$g(v_i) : (CC_{\text{NFT\_missing}}, CC_{\text{RB}}, D_{\text{O}}), \tag{9}$$

where $CC_{\text{NFT\_missing}} = \sum_{\sigma \in \textbf{CAND\_seg\_}v_i} \text{NFT}_{\text{missing},\sigma}$ is the cumulative cost of missing NFTs from v_{orig} to the actual v_i, with **CAND_seg_**v_i denoting the subset of **CAND_seg** consisting only of vertices v_{orig} to v_i and $\text{NFT}_{\text{missing},\sigma}$ denoting the $\text{NFT}_{\text{missing}}$ value for σ, i.e., the number of NFT-requested tasks that will not be computed and transmitted back to the CAV in time before t_{deadline} has passed; $CC_{\text{RB}} = \sum_{\sigma \in \textbf{CAND\_seg\_}v_i} n_{\text{RB},\sigma}$ is the total number of reserved RBs along the given vehicular route, with $n_{\text{RB},\sigma}$ being the n_{RB} value for σ; and D_{O} is the total vehicular route length from v_{orig} to the given v_i (expressed in metres).

$CC_{\text{NFT\_missing}}$ is included in the triplet, because it is one of the two key metrics considered for multiobjective optimization in this work. The reason for the inclusion of CC_{RB} in this triplet is the preference for vehicular routes that use radio resources economically. To further improve the economical use of RBs and the optimization results of our approach, the CAV is associated in a nongreedy way with the gNB that enables the CAV to fulfil $t_{\text{deadline},i}$ with the minimal number of RBs in each specific vehicular route segment. The proposed nongreedy gNB association mechanism is described in detail in subsection IV-D below. The last metric, D_O, is commonly considered in conventional applications of the A* algorithm for user/vehicle navigation.

The cost triplets of the cost function $g(.)$ are ordered lexicographically; i.e., if two triplets have n identical leftmost metric values, then the $(n+1)$-th metric serves as the tie-breaker. This property naturally gives the highest priority to the optimization of the leftmost metric in such a triplet, with decreasing importance of the subsequent metrics. In our

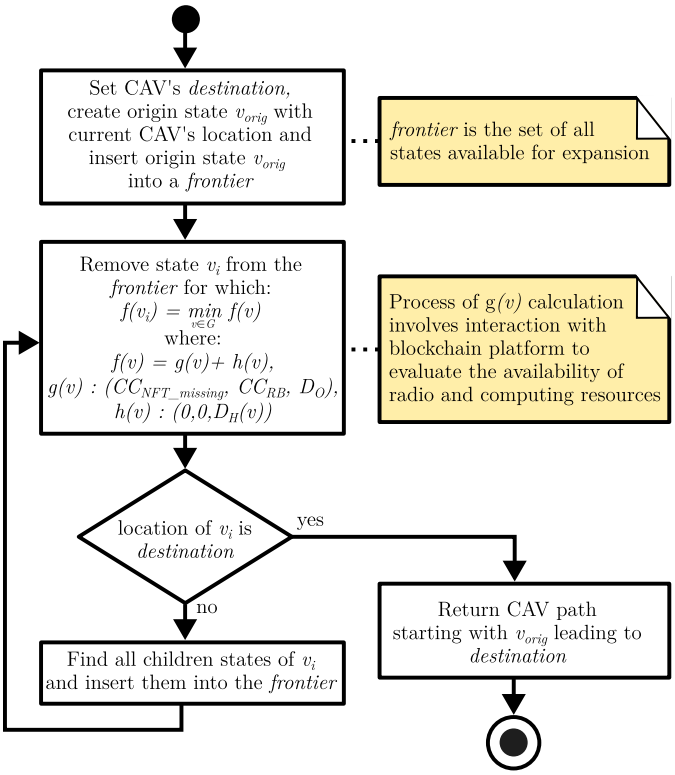

Fig. 3. Activity diagram of proposed approach based on the application of the lexicographic A* algorithm. Note that detailed interaction flow between CAV and blockchain platform (yellow note) is given in Fig. 4.

case, the highest priority in the metric tuple is assigned to $CC_{\text{NFT\_missing}}$, as this metric guarantees QoS improvement as expressed in terms of M_{FT}. The lowest priority is assigned to D_{O}, and its tradeoff with the other metrics in the cost tuple is bounded by constraint *C3* in (6).

The heuristic function $h(.)$ in a common A* search is typically a relaxation of the function $g(.)$ to balance the tradeoff between the number of $h(.)$ function calls and its computational complexity. The number of $h(.)$ function calls increases with an increasing degree of relaxation, as the quality of the route cost approximation decreases and finding the optimal route requires a more extensive search. Hence, for computing the heuristic function $h(.)$, we use a relaxed problem that fulfils the admissibility and consistency requirements for the optimality of the A* graph search. To this end, we define the heuristic function $h(.)$ based on $g(.)$, but with the two leftmost metrics set to zero, as follows:

$$h(v_i) : (0, 0, D_{\text{H}}(v_i)), \tag{10}$$

where D_{H} is the distance estimate between the given v_i and v_{destin}.

The flowchart of the proposed approach is given in Fig. 3. The flowchart illustrates the process of road segment determination based on the proposed vehicular route and resource selection algorithm. Note that detailed interaction flow between CAV and blockchain platform is presented later in Fig. 4.

D. gNB Association and Resource Allocation Mechanism

Alg. 1 describes the gNB association and resource allocation mechanism applied to assign resources to the i-th task of CAV u located in route segment σ in time interval $< t_{\text{req}}, t_{\text{rel}} >$. The required computing resources of the gNB are calculated for the i-th task as the first step of the algorithm (line 1) based on a predetermined fraction of time required for processing, $t_{\text{process},i}$, which is found as one of the hyperparameters. This hyperparameter is found through grid search [39]. The algorithm iterates through all gNBs (line 2) and chooses the CAV–gNB association that is able to fulfil the task requirements with the fewest RBs while also fulfilling the computing resource requirements. A Boolean value expressing whether the given j-th gNB fulfils the minimal task computing and radio requirements for the i-th task at time t is stored in the res_avail variable, which is used in the condition on line 3. In each search iteration, a reference to the gNB that can fulfil the task requirements with the fewest required RBs among all gNBs considered thus far is stored in best_gNB variable (line 6). Thus, this variable indicates the gNB with the absolute minimum number of RBs once the algorithm has iterated through all gNBs. The min_RB variable (line 4) stores the corresponding number of RBs provided by best_gNB. The algorithm thus assigns the specific most suitable gNB based on the fewest gNB resources that should be allocated to solve the CAV's requested task. These resources include I_i, provided by this gNB as the computing resources allocated for the i-th task, and n_RB_i, as the allocated radio resources. The gNB that is able to fulfil these task requirements in the most economical manner is associated with the CAV requesting the given task, and its gNB resources are allocated to this CAV for the necessary time interval.

To sum up the functionality of Alg. 1 from its input / output perspective, function *gNBAllocation* gets the list of independent arguments consisting of $N_{\text{gNB}}, u, i, t_{\text{req}}, t_{\text{rel}}, t_{\text{process},i}, \sigma \in$ AR_seg as its input. These represent system configuration, CAV requirements and serve for the calculation of NFT and association tuples as function output, to represent recommended resource allocation and association. Constituents of NFT tuple were already described in (7), association tuple contains u and best_gNB$_{i,k}$.

E. Network Resource Reservation Based on NFTs

Each CAV performs a separate optimization of (6) to determine the individual CAV paths, and thus, the CAVs collectively optimize the distribution of the gNBs' resources by leveraging the nongreedy resource allocation mechanism presented in Alg. 1. Note that a strictly nongreedy approach is an essential enabler of individual noncoordinated optimization by each CAV. Without the assumption of nongreediness, the noncoordinated actions of individual CAVs would mutually degrade the overall average QoS. The crucial role of blockchain is that it helps such a decentralized system control and coordinate resource utilization so as to fulfil constraints *C1* and *C2*, since both $n_{\text{RB},i}$ and I_i appear in the NFT tokens and thus limit the decentralized agreement on the planned use of resources only up to the resource limits of the individual gNBs. The blockchain mechanism also solves potential conflicts between concurrent resource requests and ensures the correct mapping of the limited gNB resources to CAVs in such cases. In addition, the blockchain mechanism guarantees gNB resource reservation, allowing collaborative

resource use planning. Thus, there is a coordinated guarantee of M_{FT} target achievement.

The process of decentralized resource allocation using the proposed blockchain-based platform is visualized in Fig. 4. Upon initialization, the AI-based vehicular route planning service running in each CAV searches for the optimal path to the desired route destination using the proposed A* variant based on the total route cost. During graph traversal by the A* algorithm, the resource availability of the corresponding gNBs is checked and booked for future utilization. Allocation of the gNB resources is executed in advance for the whole vehicular route. During the planning and allocation of the necessary available gNB resources, resources are reserved by minting NFTs that prove ownership of the given assets. After the optimal vehicular route is found, the vehicular route planning service returns the vehicular route segments coupled with the obtained required NFTs. Note that the entire planning process is executed offline, prior to the CAV departure and thus, it does not prolong the task offloading time or other performance-related metrics. In addition, due to the offline processing nature, the energy efficiency of the proposed approach differs only marginally from the current state-of-the-art methods (SQRSA and VARSA) as all communication-related aspects of CAV (radio and computing resource provisioning, signalling, etc.) remains identical during CAV travelling.

F. Computational Complexity

Now we will consider the computational complexity of our approach, by comparison with the plain A* algorithm, taking into account our modifications to its $h(.)$ and $g(.)$ functions. The worst case time complexity of plain A* algorithm searching path in a graph with average branching factor b and graph depth d is $O(b^d)$ [40].

The heuristic function $h(.)$ that calculates the distance between v_i and v_{destin} adds only a constant computation load and, thus, it can be neglected. Function $g(.)$ also adds constant computational load corresponding to obtaining both $CC_{\mathrm{NFT\_missing}}$ and CC_{RB} through information from SINR map values and information about unassigned gNB resources. These are part of the algorithm input for each CAV. Since the complexity of both functions h(.) and g(.) is negligible, the overall computation complexity of our algorithm is equal to that of the plain A* algorithm, as all of our extensions are still computationally dominated by $O(b^d)$ term.

To obtain a good estimate of algorithm runtimes in practice, that are not immediately apparent from its asymptotic complexity analysis, characteristics of typical problem instances should be considered. The average branching factor of a road network divided into a large number of segments is low, close to a value of 1, as most of the segments are not adjacent to any intersection. Runtime can be also further influenced by a suitable choice of considered graph depth d.

V. Simulation Results

We conduct Monte Carlo simulations to assess the performance of the proposed method. We vary the key parameters of the model to provide a general overview of the method's performance, including the task instruction count I_i, the task size D_i, the number of gNBs N_{gNB}, the available frequency spectrum N_{RB}, and the number of CAVs N_{CAV}. We consider a grid road topology with a size of 4.2 km^2. This choice of topology allows us to use the Manhattan distance as the heuristic function $h(.)$. Note that in the considered grid road topology model, the gNBs are located relatively close to the roadsides. In turn, gNBs are capable of taking over some of the tasks associated with autonomous driving, which are commonly handled by roadside units (RSUs). Such setup of the collocation of gNB and RSU features is already discussed, for example in [41].

The performance results of our proposed approach are obtained using simulation code that we have made available in an online GitHub repository.[1]

The key model parameters adopted in the simulation configuration are given in Table II. In addition, the considered simulation area is illustrated in Fig. 5.

Algorithm 1 CAV–gNB Association and Allocation of Radio and Computing Resources

Function *gNBAllocation*($N_{\mathrm{gNB}}, u, i, t_{\mathrm{req}}, t_{\mathrm{rel}}, t_{\mathrm{process},i}, \sigma \in$ AR_seg) **is**

/* computing resource (I_i) allocation */

1 $I_i \leftarrow I_{r,\mathrm{CPU}} * t_{\mathrm{process},i}$

$size \leftarrow D_i$

best_gNB $\leftarrow$ None

$n\_RB_i \leftarrow 0$

$min\_RB \leftarrow \infty$

$k \leftarrow \lfloor t_{\mathrm{req}}/\Delta t_{\mathrm{proc}} \rfloor$

2 **for** $j \in \{1 \ldots N_{\mathrm{gNB}}\}$ **do**

$t \leftarrow t_{\mathrm{req}}$

$temp\_RB_i \leftarrow \lceil (size/t_{\mathrm{uplink}})/(\beta_u(t)\rho_u(t)\ f_{\mathrm{s}}(t)) \rceil$

$res\_avail \leftarrow check\_resources(\mathrm{gNB}_j)$

$lowest\_RB \leftarrow temp\_RB_i < min\_RB$

3 **if** *res_avail* ***and*** *lowest_RB* **then**

4 $min\_RB \leftarrow temp\_RB_i$

/* definitive number of radio resources n_RB_i allocated after all cycle iterations */

5 $n\_RB_i \leftarrow min\_RB$

6 best_gNB$_{i,k} \leftarrow$ gNB$_j$

NFT $\leftarrow (t_{\mathrm{req}}, t_{\mathrm{rel}}, n_{\mathrm{RB},i}, I_i)$

association $\leftarrow$ (u, best_gNB$_{i,k}$)

return NFT, association;

[1]The model simulation code, including variations for the baseline methods, is available in the GitHub repository at https://github.com/AdamPetik/bc-autonomous-cars

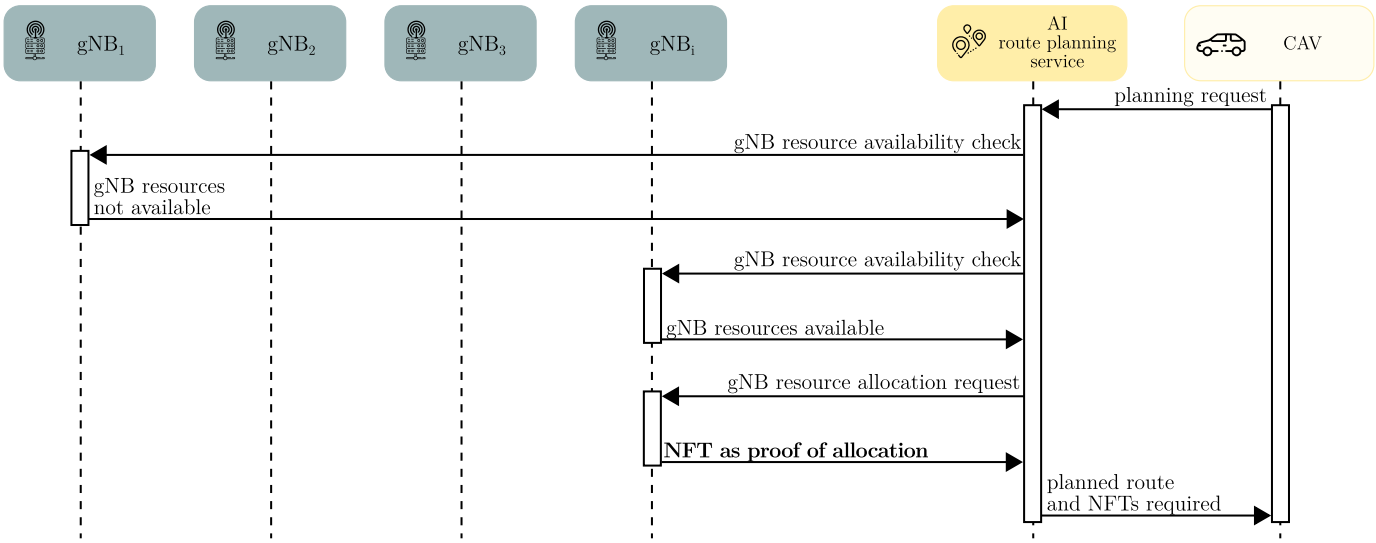

Fig. 4. Sequence diagram of the proposed blockchain-based resource allocation workflow. The CAV chooses among gNBs to manage its radio and computing requirements throughout the route planning process.

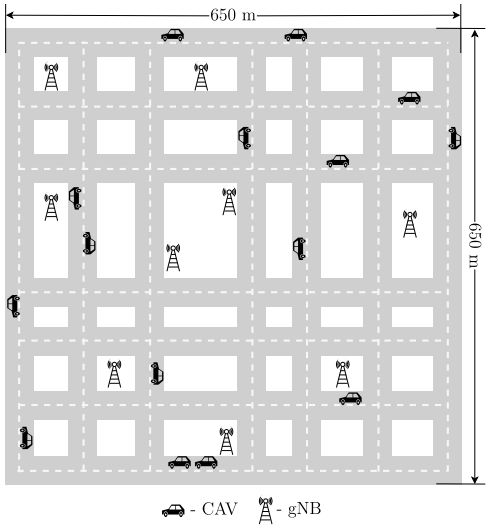

Fig. 5. Considered simulation area.

TABLE II
SIMULATION SETTINGS

Parameter	Value
N_{RB} (no. of RBs per gNB)	2000, 4000
N_{CAV} (no. of CAVs)	30, 60, 120
N_{gNB}	5, 10, 15, 20
N_{steps} (no. of simulation time steps)	1200
Simulation trial duration	6 s
v (CAV velocity)	40 km/hour
D_i	0.8, 4, 8, 16 mbits
I_i	10, 20, 40 MI
$I_{r,\mathrm{CPU}}$	$3.6 * 10^9$ IPS
Δt_{T}	0.5 s
$t_{\mathrm{process},i}$	0.1 s
gNB placement	binomial point process
CAV request activity	continuous, clocked in time steps
P_{t}	0.1 W
f_{t}	$2 * 10^9$ Hz

A. Baseline Vehicular Route Selection Scenarios

To assess the performance of the proposed method, we also apply three state-of-the-art methods for vehicular route selection and compare the results.

- FPR algorithm: selects the fastest vehicular route available to a given CAV to reach the route destination from its current location. It resembles typical vehicular route selection based on the GPS navigation system equipped on a CAV.
- SQRSA [8]: selects the vehicular route based on the available SINRs in individual vehicular route segments. The quality of the vehicular route selected in SQRSA is judged by the number of vehicular route segments that are not covered by a signal with a sufficient SINR (determined using the fixed lower threshold $th_{\mathrm{SINR}} < 5$ dB).
- VaRSA [6]: extends SQRSA, with the main difference being its additional awareness of gNB radio resource capacity.

B. Blockchain Application

To analyse the feasibility of the proposed blockchain-based framework relying on NFTs, we utilize a testnet based on the Ethereum blockchain. From a series of experiments, it is concluded that the proposed approach is technically (in the sense of smart contract/NFT deployment) applicable to the investigated CAV use case in the case of a self-customized Ethereum testnet. However, considering the massive number of CAVs that are expected to be in operation in the future, the platform's speed and latency need to be addressed prior to practical deployment. From the comparison of various blockchains given in Table III, it is evident that some widely popular solutions, such as the tested Ethereum blockchain as well as Peercoin or Hyperledger, could be easily overwhelmed by the number of transactions generated by the CAVs in the case of wide-scale implementation, thus limiting the practical applicability of our approach.

A number of distributed blockchain consensus algorithms have been proposed [42], each with a particular set of advantages and disadvantages. Although the Ethereum blockchain (with a *proof-of-work* consensus algorithm) is considered in our simulator due to the availability of a flexible

TABLE III

COMPARISON OF CONSENSUS ALGORITHMS/BLOCKCHAINS [42], [45]

Consensus algorithm/ blockchain	Number of transactions per second	Confirmation latency	Features
Proof-of-work (PoW)/ Bitcoin, Ethereum	Tens	6–60 min	High security Low throughput Low scalability
Proof-of-stake (PoS)/ Peercoin	Tens	10–60 min	High security Low throughput Low scalability
Byzantine fault tolerance (BFT)/ Hyperledger	Thousands	1–60 s	Low security High throughput High scalability
BFT-based proof-of-stake (BFT-based PoS)/ Ethereum 2.0	Thousands (if sharding used)	<1 s (within a shard)	Low security High throughput High scalability
Delegated proof-of-stake (DPoS)/ EOS, Cosmos	Thousands	<1 s	Low security High throughput High scalability
Proof-of-formulation (PoF)/ FLETA	More than 10,000	<1 s	High security High throughput High scalability

testnet, for practical deployment, we suggest using a faster blockchain infrastructure with support for smart contracts and NFTs, such as Ethereum 2.0 (*proof-of-stake*), Cosmos (*delegated proof-of-stake*) or FLETA (*proof-of-formulation*), considering the unique tradeoff between transaction time, security and scalability. It is also worth mentioning that the service and transaction costs of the deployed blockchain-based resource allocation algorithm are highly dependent on the selected blockchain infrastructure, its configuration and the underlying hardware [19].

To further improve future performance and reduce the platform latency, the utilization of *blockchain sharding* [43] appears to be a viable option in our case. This approach can be used to overcome the scalability limitations of current blockchain solutions, significantly reducing the communication overhead while maintaining the robustness and high security [44]. In contrast to the standard approach, gNBs utilizing the aforementioned sharding method are not required to maintain a full updated copy of the ledger. Instead, the gNBs are assigned to smaller groups maintaining disjoint ledgers. In our case, the formation of different groups to handle the transactions in individual cities or city districts emerges as a viable option.

C. Ratio of Failed Tasks to All Generated Tasks

We vary the available bandwidth, the number of CAVs and gNBs in Fig. 6a–6c. As the number of CAVs increases, the computing and communication requirements rise as well, resulting in an increase in M_{FT}. Fig. 6a–6c reveal that the proposed approach tends to outperform all investigated baseline methods. The relative improvements are even more significant with the increasing number of gNBs. We consider the presence of 20 and 30 gNBs in the simulations plotted in Fig. 6a, 6b and 6c. In Fig. 6a (20 gNBs, 2000 RBs), in the case of 60 CAVs in the simulation, the proposed approach reduces M_{FT} by 0.04 compared to VaRSA and provides higher gains compared to the other approaches. In addition, the performance differences are of greater interest for 120 CAVs as the proposed approach delivers even higher performance gains compared to the baselines. Fig. 6b (20 gNBs, 4000 RBs) shows similar performance between the proposed approach and the baseline methods, and the differences increase again with an increasing number of CAVs. The SQRSA and FPR curves behave very similarly, and both are significantly outperformed by both VaRSA and the proposed approach. However, the proposed approach also further outperforms VaRSA, achieving $M_{\mathrm{FT}} = 0.13$ for the scenario with 120 CAVs. This is a 31% improvement over VaRSA and a 45% improvement over SQRSA in relative terms. Fig. 6c (30 gNBs, 4000 RBs) shows performance difference trends in favour of our approach similar to those observed in Fig. 6b. The proposed approach achieves M_{FT} improvements of up to 0.05 compared to VaRSA and 0.11 compared to SQRSA, which are even more significant in relative terms (50% and 69%, respectively) than the improvements observed in the previous case.

We can draw multiple comprehensive conclusions from these three figures. First, the relative order of algorithm performance is preserved in all three figures. Additionally, the change in RB count from 2000 to 4000 is associated with less significant differences than the change in gNB count from 20 to 30 gNBs with a fixed RB count of 4000 RBs. Finally, we observe that increasing the CAV count leads to larger relative M_{FT} performance differences between the proposed algorithm and baseline algorithms.

Fig. 7a–7c demonstrate a dependency of M_{FT} on the number of gNBs (N_{gNB}) for different CAV and RB counts. The proposed approach reduces the number of gNBs in order to reach the target M_{FT}. For example, in Fig. 7c, the proposed approach requires $N_{gNB} = 16$ to reach the $M_{FT} = 0.1$, while VaRSA requires $N_{gNB} = 20$ (20% decrease in the number of required N_{gNB} introduced by the proposal relative to VaRSA) and the other baseline algorithms are not capable to deliver such low M_{FT}. This fact is of special importance for the operators, as it allows them to reduce substantially the capital expenditures (CapEx) and operating expenses (OpEx).

Finally, the dependence of M_{FT} on the task size D_i and the task instruction count measured in MI is shown in Fig. 8a–8c. M_{FT} obviously increases with an increasing task size D_i. It can be observed that the proposed approach mostly provides larger performance gains than the other three baseline methods. For example, in Fig. 8c we can observe M_{FT} increases of up to 0.06, 0.11 and 0.12 (46%, 85% and 92% relative to proposed approach), for VaRSA, SQRSA and FPR respectively, when the task size and task instruction count are higher.

D. Vehicular Route Prolongation

The vehicular route prolongation ratio (M_{RP}) is calculated as follows:

$$M_{\mathrm{RP}} = \left(\frac{T_{\mathrm{pr}}}{T_{\mathrm{FPR}}} - 1\right), \tag{11}$$

where T_{pr} is the travel time of the proposed vehicular route and T_{FPR} is the travel time of the fastest vehicular route determined via the FPR approach.

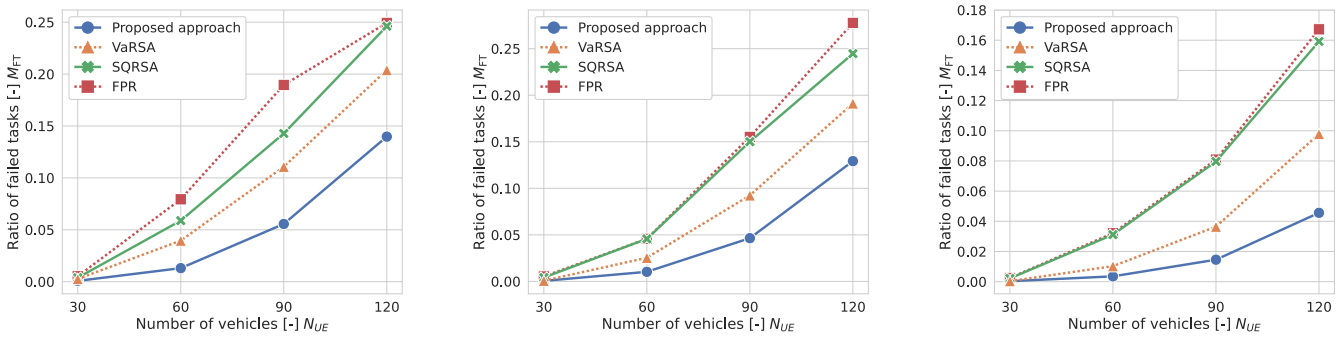

Fig. 6. Impact of number of CAVs on M_{FT} for $I_i = 40$ MI and (a) 20 gNBs and 2000 RBs of available bandwidth, (b) 20 gNBs and 4000 RBs of available bandwidth, and (c) 30 gNBs and 4000 RBs of available bandwidth.

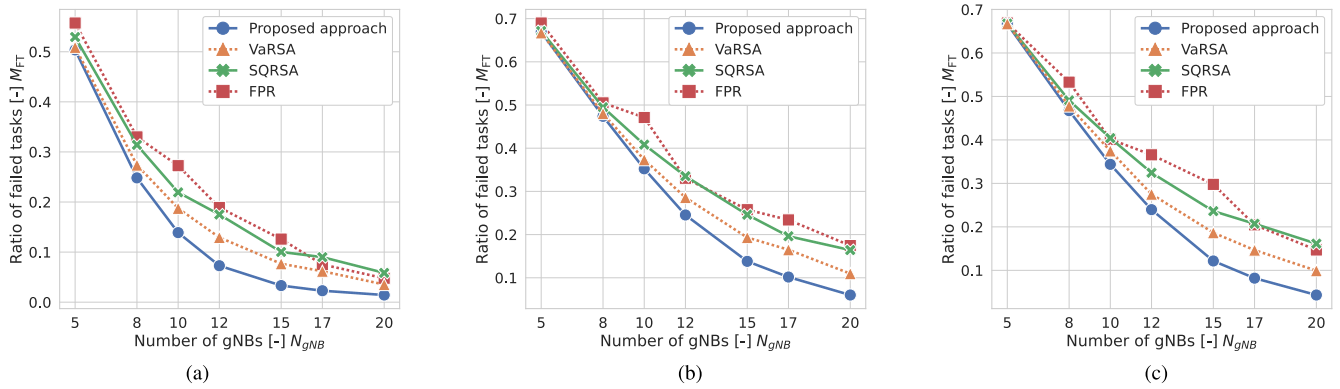

Fig. 7. Impact of the number of gNBs on M_{FT} for $I_i = 40$ MI and (a) 60 CAVs and 2000 RBs of available radio bandwidth, (b) 90 CAVs and 2000 RBs of available radio bandwidth, and (c) 90 CAVs and 4000 RBs of available radio bandwidth.

The vehicular route prolongation incurred with the considered algorithms with varying numbers of CAVs, task sizes and numbers of gNBs is presented in Fig. 9a–9c. In the case of the FPR algorithm, the planned vehicular route is also the shortest vehicular route; therefore, the prolongation is always 0. In Fig. 9a, for a low number of CAVs (0 to 80), the vehicular route prolongation of the proposed approach is lower than that of SQRSA and markedly lower than that of VaRSA. However, when the system becomes saturated (120 CAVs), the vehicular route prolongation incurred under the proposed approach is slightly higher than that of SQRSA because the more accurate allocation of the scarce gNB resources slightly prolongs the dedicated vehicular routes. Nevertheless, even in this case, the proposed approach produces routes with lengths competitive with VaRSA. Fig. 9b shows similar performance for the proposed approach and SQRSA, with M_{RP} close to 0.03. Notably, in this scenario, VaRSA statistically results in the greatest route prolongation for smaller task sizes. Moreover, for a varying number of gNBs (Fig. 9c), similar conclusions can be drawn, i.e., the proposed method and SQRSA shorten the vehicular routes compared to VaRSA. The route prolongation gap between our approach and VaRSA increases with the growing gNB count.

E. Model Limitations and Possible Extensions

The numerical experiments presented in this section suggest that the proposed model provides in general significant performance gains compared to the state-of-the-art algorithms. However, we should mention a few relaxing assumptions in our model. We assume perfect time synchronization (for example, in terms of CAV speed predictability) and no unpredictable situations in traffic (road accidents, people on crosswalks, etc.), respectively. These relaxing assumptions may not be always valid in practice. On the one hand, such non-deterministic events creating irregularities in the traffic would trigger the NFT exchange between the CAVs to adapt to the new road conditions, allowing seamless services to be provided. On the other hand, such new transactions could create an additional load on the underlying blockchain platform, prolonging the time required for the transaction consensus. The transaction in terms of the NFT exchange among the CAVs is a complex problem due to the non-deterministic character of the events occurring in the traffic, hence, we leave it out for future research.

Another class of unpredictable events, which would be an interesting addition to our model, are transient and persistent failures of the network, and computational resources caused either by hardware or software malfunction. These could be solved by various approaches, like secure microservice-based architecture with deadline-aware fault resolution algorithm shown in [46].

An alternative approach to deterministic trajectory planning is a probabilistic model obtained using mobility data mining. Such data should be obtained with proper encryption and anonymization of the data, such as the approach presented in [47]. The introduction of this probabilistic model would cause changes requiring the replacement of A* search, as no universally applicable probabilistic variants of this algorithm exist. However, A* search with a suitable heuristic function

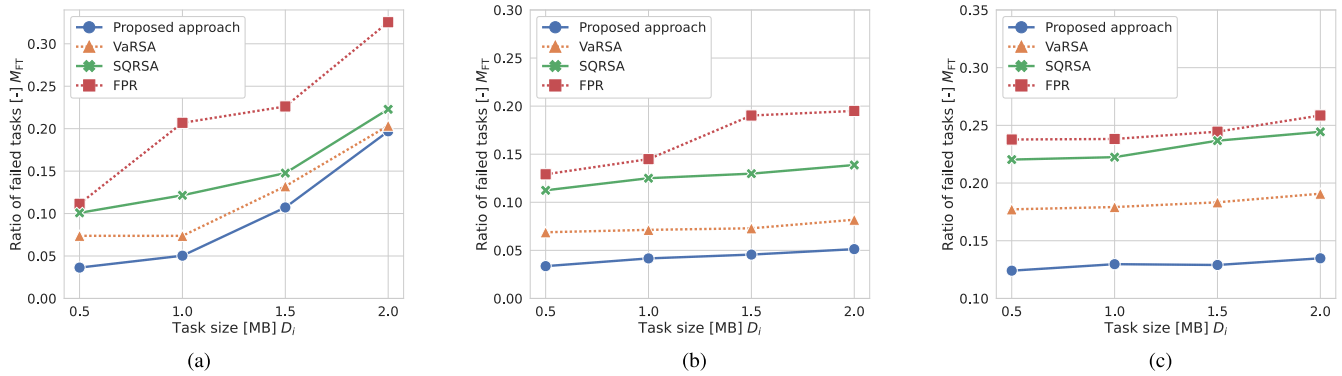

Fig. 8. Impact of task size on M_{FT} in several simulated scenarios: (a) 60 CAVs, 30 MI tasks and 2000 RBs of radio bandwidth; (b) 60 CAVs, 30 MI tasks and 4000 RBs of radio bandwidth; and (c) 60 CAVs, 40 MI tasks and 4000 RBs of radio bandwidth.

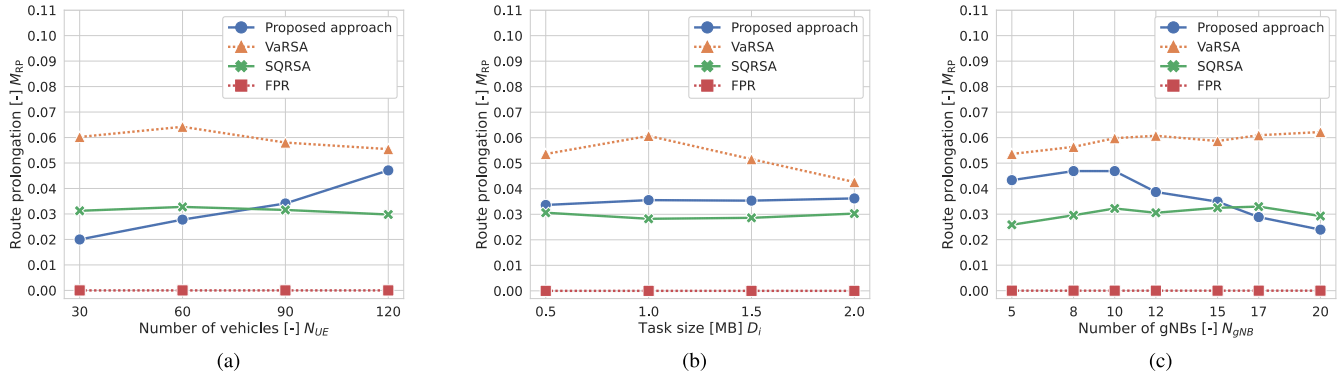

Fig. 9. Ratio of vehicular route prolongation relative to the shortest vehicular route with (a) a varying number of CAVs in the same simulation configuration as in Fig. 6b, (b) a varying task size in the same simulation configuration used in Fig. 8b; and (c) a varying number of gNBs with I = 40 MI, 60 CAVs and 4000 RBs of available radio bandwidth.

allows us to predict provably optimal CAV trajectories, of perfectly predictably moving CAVs. In environments with a low number of unexpected events, a deterministic approach with occasional replanning yields near-optimal path planning results. Apart from this advantage, the added benefit of a near-deterministic environment is a very low number of incorrect resource allocation assignments, which would plague even optimal models working with stochastic environments.

Another possible extension beyond the current scope of our work is a complex resource scheduling considering trade-off management, with a strong emphasis on security and privacy, as presented in [48] and [49].

VI. Conclusion

In this paper, a novel vehicular route selection algorithm based on the joint reservation of radio and computing resources in MEC is proposed. The proposed algorithm exploits the ability to account for the future locations of CAVs and the CAV service requirements. For this purpose, a decentralized blockchain platform supporting the transfer of NFTs among autonomous CAVs is designed. Each NFT represents the equivalent radio resources of the mobile network infrastructure and the computing resources of a gNB reserved for the CAV in a given time interval and road segment. The proposed approach is proven to be more effective than state-of-the-art approaches in terms of M_{FT} and M_{RP} in a number of different scenarios.

Further research in this area can be viewed in the context of various smart city applications related to autonomous driving, such as car sharing, robotic delivery systems, and public transportation. Considering the relation between network congestion and the number of CAVs, the findings of the current paper can also motivate new research on road traffic congestion control. Another promising direction of investigation would be the consideration of vehicle-to-vehicle (V2V) communications integrated with our approach.

Appendix

A. Proof of the Consistency of the Proposed A* Heuristic

To prove that the heuristic function of the proposed A* path-finding algorithm is consistent, it is necessary to show that it has the triangle inequality property and evaluates to 0 at the target route destination vertex v_{destin} [40], as expressed in (12):

$$\begin{aligned} h(v_i) &\leq c(v_i, v_{desc}) + h(v_{desc}) \\ h(v_{destin}) &= 0, \end{aligned} \tag{12}$$

where v_{desc} is any vertex subsequent to the given v_i, h is the heuristic function given in (10) and $c(v_i, v_{desc})$ is the cost of reaching v_{desc} from the given v_i expressed as a tuple of the form $(CC_{NFT\_missing}, CC_{RB}, distance)$.

The values of $CC_{NFT\_missing}$ and CC_{RB} are always 0; these components of the cost tuple thus satisfy the triangle inequality property, and it remains only to show that the distance tuple component does also. For this purpose, the distance D_M between the given v_i and v_{destin} needs to be calculated. In the grid-aligned graph considered in our scenario, D_M is the shortest possible distance of a vehicular route between any node pair, and its estimate is thus always $\leq c(.)$. Therefore,

the distance component also satisfies Eq. (12), as $h(v_i) - h(v_{\text{desc}}) \leq c(v_i, v_{\text{desc}})$.

REFERENCES

[1] D. P. M. Osorio et al., "Towards 6G-enabled internet of vehicles: Security and privacy," *IEEE Open J. Commun. Soc.*, vol. 3, pp. 82–105, 2022.

[2] N. A. Zardari, R. Ngah, O. Hayat, and A. H. Sodhro, "Adaptive mobility-aware and reliable routing protocols for healthcare vehicular network," *Math. Biosci. Eng.*, vol. 19, no. 7, pp. 7156–7177, 2022.

[3] G.-P. Antonio and C. Maria-Dolores, "Multi-agent deep reinforcement learning to manage connected autonomous vehicles at tomorrow's intersections," *IEEE Trans. Veh. Technol.*, vol. 71, no. 7, pp. 7033–7043, Jul. 2022.

[4] S. Wijethilaka and M. Liyanage, "Survey on network slicing for Internet of Things realization in 5G networks," *IEEE Commun. Surveys Tuts.*, vol. 23, no. 2, pp. 957–994, 2nd Quart., 2021.

[5] Y. Ma, H. Wang, J. Xiong, J. Diao, and D. Ma, "Joint allocation on communication and computing resources for fog radio access networks," *IEEE Access*, vol. 8, pp. 108310–108323, 2020.

[6] M. Vondra, Z. Becvar, and P. Mach, "Vehicular network-aware route selection considering communication requirements of users for ITS," *IEEE Syst. J.*, vol. 12, no. 2, pp. 1239–1250, Jun. 2018.

[7] A. H. Sodhro, S. Pirbhulal, Z. Luo, K. Muhammad, and N. Z. Zahid, "Toward 6G architecture for energy-efficient communication in IoT-enabled smart automation systems," *IEEE Internet Things J.*, vol. 8, no. 7, pp. 5141–5148, Apr. 2021.

[8] M. Vondra, S. Djahel, and J. Murphy, "VANETs signal quality-based route selection in smart cities," in *Proc. IFIP Wireless Days (WD)*, Nov. 2014, pp. 1–8.

[9] B. Chen, Q. Yuan, J. Li, J. Lu, and B. Zhu, "Joint route planning and traffic signal timing for connected vehicles: An edge cloud enabled multi-agent game method," in *Proc. Int. Conf. Space-Air-Ground Comput. (SAGC)*, Dec. 2020, pp. 1–6.

[10] O. Zhdanenko et al., "Demonstration of mobile edge cloud for 5G connected cars," in *Proc. 16th IEEE Annu. Consum. Commun. Netw. Conf. (CCNC)*, Jan. 2019, pp. 1–2.

[11] Q. You and B. Tang, "Efficient task offloading using particle swarm optimization algorithm in edge computing for industrial Internet of Things," *J. Cloud Comput.*, vol. 10, no. 1, pp. 1–11, Dec. 2021.

[12] N. Cha, C. Wu, T. Yoshinaga, Y. Ji, and K.-L.-A. Yau, "Virtual edge: Exploring computation offloading in collaborative vehicular edge computing," *IEEE Access*, vol. 9, pp. 37739–37751, 2021.

[13] X. Li, Y. Dang, M. Aazam, X. Peng, T. Chen, and C. Chen, "Energy-efficient computation offloading in vehicular edge cloud computing," *IEEE Access*, vol. 8, pp. 37632–37644, 2020.

[14] X. Huang, R. Yu, D. Ye, L. Shu, and S. Xie, "Efficient workload allocation and user-centric utility maximization for task scheduling in collaborative vehicular edge computing," *IEEE Trans. Veh. Technol.*, vol. 70, no. 4, pp. 3773–3787, Apr. 2021.

[15] B. Lin, X. Zhou, and J. Duan, "Dimensioning and layout planning of 5G-based vehicular edge computing networks towards intelligent transportation," *IEEE Open J. Veh. Technol.*, vol. 1, pp. 146–155, 2020.

[16] S. Malik, V. Dedeoglu, S. S. Kanhere, and R. Jurdak, "TrustChain: Trust management in blockchain and IoT supported supply chains," in *Proc. IEEE Int. Conf. Blockchain (Blockchain)*, Jul. 2019, pp. 184–193.

[17] G. S. Aujla, A. Singh, M. Singh, S. Sharma, N. Kumar, and K.-K.-R. Choo, "BloCkEd: Blockchain-based secure data processing framework in edge envisioned V2X environment," *IEEE Trans. Veh. Technol.*, vol. 69, no. 6, pp. 5850–5863, Jun. 2020.

[18] S. Kim and A. S. Ibrahim, "Byzantine-fault-tolerant consensus via reinforcement learning for permissioned blockchain-empowered V2X network," *IEEE Trans. Intell. Vehicles*, vol. 8, no. 1, pp. 172–183, Jan. 2023.

[19] M. Salimitari, M. Joneidi, and Y. P. Fallah, "BATS: A blockchain-based authentication and trust management system in vehicular networks," in *Proc. IEEE Int. Conf. Blockchain (Blockchain)*, Dec. 2021, pp. 333–340.

[20] J. Shi, J. Du, Y. Shen, J. Wang, J. Yuan, and Z. Han, "DRL-based V2V computation offloading for blockchain-enabled vehicular networks," *IEEE Trans. Mobile Comput.*, early access, Feb. 23, 2022, doi: 10.1109/TMC.2022.3153346.

[21] S. Islam, S. Badsha, S. Sengupta, H. La, I. Khalil, and M. Atiquzzaman, "Blockchain-enabled intelligent vehicular edge computing," *IEEE Netw.*, vol. 35, no. 3, pp. 125–131, May 2021.

[22] H. Liu, P. Zhang, G. Pu, T. Yang, S. Maharjan, and Y. Zhang, "Blockchain empowered cooperative authentication with data traceability in vehicular edge computing," *IEEE Trans. Veh. Technol.*, vol. 69, no. 4, pp. 4221–4232, Apr. 2020.

[23] Y. Lu et al., "Accelerating at the edge: A storage-elastic blockchain for latency-sensitive vehicular edge computing," *IEEE Trans. Intell. Transp. Syst.*, vol. 23, no. 8, pp. 11862–11876, Aug. 2022.

[24] Z. Wang, W. Zhang, B. Liu, D. Jiang, F. Wang, and J. Zhang, "A joint and dynamic routing approach to connected vehicles via LEO constellation satellite networks," *Wireless Netw.*, pp. 1–13, Sep. 2021.

[25] M. Vallati, E. Scala, and L. Chrpa, "A hybrid automated planning approach for urban real-time routing of connected vehicles," in *Proc. IEEE Int. Intell. Transp. Syst. Conf. (ITSC)*, Sep. 2021, pp. 3821–3826.

[26] Q. Yuan, B. Chen, G. Luo, J. Li, and F. Yang, "Integrated route planning and resource allocation for connected vehicles," *China Commun.*, vol. 18, no. 3, pp. 226–239, Mar. 2021.

[27] 3GPP, *NR; Physical Channels and Modulation*, 3rd Generation Partnership Project (3GPP), Technical Specification, document (TS) 38.211, Apr. 2017, version 15.10.0. [Online]. Available: https://portal.3gpp.org/desktopmodules/Specifications/SpecificationDetails.aspx?specificationId=3213

[28] Y. Mao, J. Zhang, Z. Chen, and K. B. Letaief, "Dynamic computation offloading for mobile-edge computing with energy harvesting devices," *IEEE J. Sel. Areas Commun.*, vol. 34, no. 12, pp. 3590–3605, Dec. 2016.

[29] F. Yu, M. Ma, and X. Li, "A blockchain-assisted seamless handover authentication for V2I communication in 5G wireless networks," in *Proc. IEEE Int. Conf. Commun. (ICC)*, Jun. 2021, pp. 1–6.

[30] W. Crowe and T. T. Oh, "Distributed unit security for 5G base-stations using blockchain," in *Proc. Int. Conf. Softw. Secur. Assurance (ICSSA)*, Oct. 2020, pp. 10–14.

[31] L. Xie, Y. Ding, H. Yang, and X. Wang, "Blockchain-based secure and trustworthy Internet of Things in SDN-enabled 5G-VANETs," *IEEE Access*, vol. 7, pp. 56656–56666, 2019.

[32] M. Hojjati, A. Shafieinejad, and H. Yanikomeroglu, "A blockchain-based authentication and key agreement (AKA) protocol for 5G networks," *IEEE Access*, vol. 8, pp. 216461–216476, 2020.

[33] I. Makhdoom, M. Abolhasan, H. Abbas, and W. Ni, "Blockchain's adoption in IoT: The challenges, and a way forward," *J. Netw. Comput. Appl.*, vol. 125, pp. 251–279, Jan. 2019.

[34] W. Entriken, S. Dieter, J. Evans, and N. Sachs. (Jan. 2018). *EIP-721: Non-Fungible Token Standard*. [Online]. Available: https://eips.ethereum.org/EIPS/eip-721

[35] Q. Wang, R. Li, Q. Wang, and S. Chen, "Non-fungible token (NFT): Overview, evaluation, opportunities and challenges," 2021, *arXiv:2105.07447*.

[36] Z. Zheng et al., "An overview on smart contracts: Challenges, advances and platforms," *Future Gener. Comput. Syst.*, vol. 105, pp. 475–491, 2020.

[37] J. S. Arora, "Multi-objective optimum design concepts and methods," in *Introduction to Optimum Design*, 3rd ed., J. S. Arora, Ed. Boston, MA, USA: Academic, 2012, ch. 17, pp. 657–679. [Online]. Available: https://www.sciencedirect.com/science/article/pii/B9780123813756000176

[38] C. Sun, S. G. Ritchie, K. Tsai, and R. Jayakrishnan, "Use of vehicle signature analysis and lexicographic optimization for vehicle reidentification on freeways," *Transp. Res. C, Emerg. Technol.*, vol. 7, no. 4, pp. 167–185, Aug. 1999.

[39] M. Feurer and F. Hutter, "Hyperparameter optimization," in *Automated Machine Learning*. Cham, Switzerland: Springer, 2019, pp. 3–33.

[40] S. Russell and P. Norvig, *Artificial Intelligence: A Modern Approach*. Harlow, U.K.: Pearson, 2002.

[41] S. Zeadally, M. A. Javed, and E. B. Hamida, "Vehicular communications for ITS: Standardization and challenges," *IEEE Commun. Stand. Mag.*, vol. 4, no. 1, pp. 11–17, Dec. 2020.

[42] Y. Xiao, N. Zhang, W. Lou, and Y. T. Hou, "A survey of distributed consensus protocols for blockchain networks," *IEEE Commun. Surveys Tuts.*, vol. 22, no. 2, pp. 1432–1465, 2nd Quart., 2020.

[43] H. Dang, T. T. A. Dinh, D. Loghin, E.-C. Chang, Q. Lin, and B. C. Ooi, "Towards scaling blockchain systems via sharding," in *Proc. Int. Conf. Manage. Data*, New York, NY, USA, Jun. 2019, pp. 123–140, doi: 10.1145/3299869.3319889.

[44] M. Zamani, M. Movahedi, and M. Raykova, "Rapidchain: Scaling blockchain via full sharding," in *Proc. ACM SIGSAC Conf. Comput. Commun. Secur.*, 2018, pp. 931–948.

[45] G. Yu, X. Wang, K. Yu, W. Ni, J. A. Zhang, and R. P. Liu, "Scaling-out blockchains with sharding: An extensive survey," in *Blockchains for Network Security: Principles, Technologies and Applications* (Computing). London, U.K.: Institution of Engineering and Technology, 2020, pp. 225–270, doi: 10.1049/PBPC029E_ch10.

[46] A. H. Sodhro, A. Lakhan, S. Pirbhulal, T. M. Groenli, and H. Abie, "A lightweight security scheme for failure detection in microservices IoT-edge networks," in *Sensing Technology*. Cham, Switzerland: Springer, 2022, pp. 397–409.
[47] R. Talat, M. S. Obaidat, M. Muzammal, A. H. Sodhro, Z. Luo, and S. Pirbhulal, "A decentralised approach to privacy preserving trajectory mining," *Future Gener. Comput. Syst.*, vol. 102, pp. 382–392, Jan. 2020.
[48] A. Lakhan et al., "Cost-efficient service selection and execution and blockchain-enabled serverless network for Internet of Medical Things," *Math. Biosci. Eng.*, vol. 18, no. 6, pp. 7344–7362, 2021.
[49] A. H. Sodhro, S. Pirbhulal, M. Muzammal, and L. Zongwei, "Towards blockchain-enabled security technique for industrial Internet of Things based decentralized applications," *J. Grid Comput.*, vol. 18, no. 4, pp. 615–628, Dec. 2020.

Marcel Vološin received the M.Sc. and Ph.D. degrees in informatics from the Department of Computers and Informatics, Technical University of Košice, Slovakia, in 2018 and 2021, respectively. Currently, he is an Assistant Professor in informatics with the Department of Computers and Informatics. His research interests include agent-based real-time spectrum sharing schemes and wireless networks in conjunction with blockchain technology and mobility models in a simulated city environment.

Eugen Šlapak is currently an Assistant Professor with the Technical University of Košice, Slovakia. His Ph.D. thesis focused on HetNet physical topology design under the supervision of Prof. Juraj Gazda. He works with the research team at the university's Intelligent Information Systems Laboratory (http://iislab.kpi.fei.tuke.sk/). His research interests include radio access network simulation, optimization, and machine learning.

Zdenek Becvar (Senior Member, IEEE) received the M.Sc. and Ph.D. degrees in telecommunication engineering from Czech Technical University (CTU) in Prague, Czech Republic, in 2005 and 2010, respectively. He is currently an Associate Professor with the Department of Telecommunication Engineering, Czech Technical University in Prague. From 2006 to 2007, he joined the Sitronics Research and Development Center, Prague, focusing on speech quality in VoIP. Furthermore, he was involved in research activities of the Vodafone Research and Development Center, CTU in Prague, in 2009. He was on internships with Budapest Politechnic, Hungary (2007), CEA-Leti, France (2013), and EURECOM, France (2016 and 2019). From 2013 to 2017, he was a representative of CTU in Prague in ETSI and 3GPP standardization organizations, where he founded laboratory of mobile networks—6Gmobile research laboratory—focusing on future mobile networks. He has published more than 100 conferences or journal papers. He works on development of solutions for future mobile networks with a special focus on optimization of mobility and radio resource management, energy efficiency, device-to-device communication, edge computing, C-RAN, self-optimization, and architecture of radio access networks. He servers as an Editor for IEEE WIRELESS COMMUNICATIONS LETTERS.

Taras Maksymyuk (Member, IEEE) received the Ph.D. degree in telecommunication systems and networks from Lviv Polytechnic National University, Lviv, Ukraine, in 2015. He is currently a Research Professor with the Telecommunications Department, Lviv Polytechnic National University. He did his post-doctoral fellowship with the Internet of Things and Artificial Intelligence Laboratory, Korea University. His research interests include 5G heterogeneous networks, software-defined networks, the Internet of Things, blockchain, big data, and artificial intelligence. He is currently an Associate Editor of *IEEE Communications Magazine* and an Editor of *Wireless Communications and Mobile Computing*.

Adam Petík is currently pursuing the master's degree in informatics with the Department of Computers and Informatics, Technical University of Košice. He is one of the premier students in his year and received a letter of recognition from Huawei for his bachelor's thesis.

Madhusanka Liyanage (Senior Member, IEEE) received the B.Sc. degree (Hons.) in electronics and telecommunication engineering from the University of Moratuwa, Moratuwa, Sri Lanka, in 2009, the M.Eng. degree from the Asian Institute of Technology, Bangkok, Thailand, in 2011, the M.Sc. degree from the University of Nice Sophia Antipolis, Nice, France, in 2011, and the Doctor of Technology degree in communication engineering from the University of Oulu, Oulu, Finland, in 2016. From 2011 to 2012, he worked as a Research Scientist with the I3S Laboratory and Inria, Shopia Antipolis, France. He is currently an Assistant Professor and an Ad Astra Fellow with the School of Computer Science, University College Dublin, Ireland. He is also acting as an Adjunct Professor with the Center for Wireless Communications, University of Oulu. From 2015 to 2018, he was a Visiting Research Fellow with CSIRO, Australia; Infolabs21, Lancaster University, U.K.; the School of Computer Science and Engineering, University of New South Wales, Australia; the School of IT, University of Sydney, Australia; LIP6, Sorbonne University, France; and the Department of Computer Science, University of Oxford, U.K. His research interests lie in 5G/6G networking, SDN, the IoT, blockchain, MEC, and mobile and virtual network security.

In 2020, he received the "2020 IEEE ComSoc Outstanding Young Researcher" Award from IEEE ComSoc EMEA. He was a recipient of the prestigious Marie Skłodowska-Curie Actions Individual Fellowship from 2018 to 2020. For more information visit the link (www.madhusanka.com).

Juraj Gazda has been a Guest Researcher with Ramon Llull University, Barcelona, and the Technical University of Hamburg, Harburg. He is currently a Professor with the Faculty of Electrical Engineering, Technical University of Košice (TUKE), Slovakia. He has been involved in development with Nokia Siemens Networks (NSN). In 2017, he was recognized as the Best Young Scientist with TUKE. Currently, he serves as an Editor of *KSII Transactions on Internet and Information Systems* and a Guest Editor of *Wireless Communications and Mobile Computing* (Wiley). His research interests include spectrum pricing, techno-economic aspects of 5G networks, the coexistence of HetNets, and machine learning in 5G networks.